# Lanthanide [Terbium (III)] doped molecularly imprinted nano-architectures for the fluorimetric detection of melatonin

Erdoğan Özgür[1,2], Hirak K. Patra[3,4], Anthony P. F. Turner[5], Adil Denizli[2], Lokman Uzun[2]*

[1] Advanced Technologies Application and Research Center, Hacettepe University, Ankara, Turkey

[2] Department of Chemistry, Faculty of Science, Hacettepe University, Ankara, Turkey

[3] Department of Clinical and Experimental Medicine, Linkoping University, Linkoping, Sweden

[4] Department of Chemical Engineering and Biotechnology, University of Cambridge, Cambridge, UK

[5] Professor Emeritus, SATM, Cranfield University, Bedfordshire, UK

## Abstract

Polymerisable terbium(III) complex-based fluorescent molecular imprinted smart nanoparticles were synthesised for the quantitative determination of potential metabolic destitution biomarkers. Melatonin has been reported to one of the key factors in Seasonal Affective Disorder (SAD) and was chosen as a model metabolite to demonstrate a novel MIP nanoparticle sensor. We exploited lanthanide ion complexes in our biosensing platforms due to their deeper penetration ability, negligible auto-fluorescence, lack of photo bleaching and photo blinking, and their sharp absorption and emission bands, extreme photo stability, and long lifetime. Given the high affinity of lanthanide ions for carboxylic acid groups, we used two amino acid-based functional monomers, N-methacryloyl-L-tryptophan and N-methacryloyl-L-aspartic acid, to coordinate terbium(III) ions and melatonin, respectively. The fluorescent MIP nanoparticles were synthesised using a miniemulsion polymerisation technique after forming complexes between terbium(III):MA-Asp and melatonin:MATrp molecules. Due to the polymerisability of lanthanide complexes, they were readily inserted into the polymeric chain, which enabled homogeneous distribution as well as closer orientation to the imprinted cavities for selective melatonin recognition.

**Keywords:** Lantanite ions, molecular imprinting, fluorescent molecular imprinted nanoparticles.

***Corresponding author:**

**L. Uzun, Prof. Dr.**

Department of Chemistry, Faculty of Science, Hacettepe University, Ankara, Turkey

E-mail: lokman@hacettepe.edu.tr; Tel: +90312 297 7337

## Introduction

Lanthanide based luminescent nanoparticles (NPs) are promising alternative to fluorescent quantum dots (QDs) and organic dyes.[1] The weak photostability (photobleaching in a few minutes on exposure to light), low quantum yield, narrow excitation bands, broad emission bands, lifetime of 1-5 s, and small Stokes shifts[2] have limited the biological application of traditional organic dyes. QDs are also known as semiconductor nanocrystals and endow unique optical properties such as better chemical stability, a wide excitation range, a narrow emission band, and resistance to photobleaching, and thus overcome some of the deficiencies of organic dyes.[3] However, potential toxicity due to having heavy metal ions in their structures (CdSe, CdS),[4] solubility in aqueous and biologically environments and complicated bio-functionalisation strategies have also limited their use in biological applications as fluorescent probes.[3,5,6,7] These drawbacks of organic dyes and QDs have led the researchers to investigate novel compounds such as lanthanide ions. Lanthanide ions ($Ln^{3+}$) possess long luminescence lifetimes (~1 ms), which enables time resolved detection,[8] in view of the formally forbidden 4f–4f electronic transitions, compared to organic dyes. Emission wavelengths of lanthanides also alter over a small range, because the 4f orbitals don't straightly contribute to bonding due to shielding effect of the 5s and 5p orbitals, so the energy level of these orbitals are not affected by the surrounding environment (or matrix) and nanoparticle size.[9,10] Hence, the absorption bands (1-5 nm broad), narrow emission bands (10 nm broad) and large effective Stokes shifts (~150 nm for $YVO_4$:Eu NPs)[11] of lanthanide ions attract considerable interest in their use as luminescence probes and labels for applications in imaging and sensing.[9,12-14] Terbium (III) and Europium (III) have been broadly researched for biosensing in analytical/bioanalytical applications.[1,15]

The combination of lanthanide ions (or their complexes) and NPs to create novel hybrid nanomaterials has received much attention in research fields such as sensing, biomedical imaging and drug delivery etc.[16] Incorporation of lanthanide ions into molecularly imprinted polymeric materials can provide specific binding events for many biomedical and diagnostic analyses.[1,17] Such multifunctional nanostructures based on the molecular imprinting technique offering specific biorecognition with fluorescent emission have been consider as a new class of researcher in the last years. [18-20]

Molecular imprinting mimics the specific biorecognition ability of biological systems by using polymeric structures with similar interactions.[21,22] Molecularly imprinted polymeric materials are generally produced by bulk polymerisation, but disadvantages such as the relatively low number of binding sites near the surface, heterogeneity in binding affinity, low rebinding capacity and slow rebinding kinetics limit their application in molecular diagnostics at the nanoscale.[23-25] So, NPs with the high surface area to volume ratio, high binding afinity/capacity, and relatively high mass transfer due to binding position being on or near the surface compared with traditional molecularly imprinted materials, have attracted attention for molecular recognation at the nanoscale.[23] Molecularly imprinted luminescent nanocomposites can be produced by using fluorescent monomers during the synthesis process of molecularly imprinted polymers,[26] copolymerisation of fluorescent nanomaterials like QDs, lanthanide doped NPs, fluorescent dyes, cross linkers and target analyte (synthesis of molecularly imprinted structures occurs by copolymerisation of functional monomers, cross-linkers in the presence of analyte)[27] and encapsulation strategies.[28]

Briefly, polymerisable terbium(III) complex-based fluorescent MIP NPs have been synthesised for the quantitative determination of potential metabolic biomarkers. The melatonin molecule has been chosen as a model metabolite to demonstrate this MIP nanoparticle sensor. Melatonin is part of the metabolic pathway of L-tryptophan and has been reported to one of the key factors in seasonal affective disorder (SAD).[29] Melatonin can be determined by HPLC with fluorescence, mass spectrometry, GC and MS, radioimmunoassay, ELISA, electrochemical sensing and immunoprecipitation. However, there is an unmet need for a simple, inexpensive sensor-based system for use in point-of-care applications. Herein, we have exploited lanthanide ion complexes in our biosensing platforms due to their deeper penetration ability, negligible auto-fluorescence, lack of photo bleaching and photo blinking, and their sharp absorption and emission bands, long lifetime and extreme photo stability. It is known that carboxyl groups of amino acids serving as chelates are particularly suitable ligands with high affinity.[30-32] Two amino acid-based polymerisable functional monomers, N-methacryloyl-L-aspartic acid (MAAsp) and N-methacryloyl-L-tryptophan (MATrp) **(Figure S1)** were synthesised to coordinate terbium(III) ions and melatonin, respectively. The fluorescent MIP NPs were synthesised using micro-emulsion polymerisation techniques after forming complexes between terbium(III):MAAsp and melatonin:MATrp molecules. Due to the polymerisability of lanthanide complexes, they were readily inserted into the polymeric chain, which enabled homogeneous distribution as well as closer orientation to the imprinted cavities for selective melatonin recognition. By this approach, we aimed to developed an alternative nanoparticle-based sensor system that has advantages to commercially available melatonin detection method.

## 2. Experimental

### 2.1. Chemicals

L-tryptophan, L-aspartic acid, terbium(III) nitrate pentahydrate, 2-hydroxyethyl methacrylate (98%) (HEMA), poly(vinyl alcohol) (PVA), ethylene glycol dimethacrylate (EGDMA), α,α'-azoisobutyronitrile (AIBN), 1H-benzotriazole, triethylamine (≥99.5%), methacryloyl chloride (≥97%), sodium bicarbonate, ammonium persulfate, sodium bisulfite, sodium dodecyl sulfate (SDS), melatonin and serotonin hydrochloride were were supplied by Sigma Chemical Co. (St. Louis, USA).

### 2.2. Synthesis of MAAsp and MATrp functional monomers

Amino acid based functional monomers, MAAsp and MATrp were prepared as previously described with minor modifications[33]. 5.52 mmol of amino acid (L-aspartic acid or L-tryptophan) was dissolved in 1 M aqueous solution of NaOH. The solution of benzotriazole methacrylate (MA-Bt) (5.52 mmol) in 25 mL of 1,4-dioxane was added to the amino acid solution and continuously stirred at room temperature for 30 min. The, the 1,4-dioxane was evaporated under vacuum. The residue was diluted with DI water and extracted with ethyl acetate to remove 1H-benzotriazole. Then, water was evaporated to obtain MAAsp and MATrp.

### 2.3. Synthesis of Fluorescent Tb(III):MAAsp Complex

The fluorescent complex was prepared using N-methacryloyl-L-aspartic acid (MAAsp) and Tb(III), in 3:1 molar ratio as [Tb(III):MAAsp]. Lanthanide ions make several coordination complexes with nitrogen- and oxygen-rich ligands. Most complexes of lanthanide ions with biomolecules are formed via nonadentate interactions.[34, 35] So, it was chosen the molar ratio of [Tb(III): MAAsp] as 3:1 due to three carboxyl groups of the MAAsp monomer. In brief, MAAsp (3 mmol) and ammonium oxalate monohydrate (0.5 mmol) dissolved in deionized water (DI). pH was fixed up between 6.0-7.0 for the complexation and 1 mmol of $Tb(NO_3)_3.5H_2O$ was added under magnetically stirring at 200 rpm for 12 h, then, the white precipitate was taken from solution. Characterisation of the complex was done by spectrofluorimetric measurements (Shimadzu, RF 5301, Tokyo, Japan).

### 2.4. Synthesis of Molecularly Imprinted Fluorescent Nanoparticles (NPs)

Two-phase miniemulsion polymerisation was performed for the synthesis of melatonin imprinted fluorescent NPs. SDS (15.0 mg, surfactant forming emulsion), PVA (93.0 mg, surfactant stabilizing unsaturated polymer chain), and sodium bicarbonate (12.50 mg) were dissolved in 5.0 mL of DI for phase 1. SDS (50.0 mg) and PVA (50.0 mg) were dissolved in 100.0 mL of DI for phase 2. Phase 3 (organic phase) was formed by mixing MATrp (0.125 mmol, functional monomer), HEMA (0.50 mmol, monomer) and EDMA (15.0 mmol, cross-linker). Phase 3 was slowly added to phase 1. The mixture was homogenised at 25000 rpm to obtain miniemulsion. Then, template molecule (melatonin) (0.125 mmol) was added to the miniemulsion and mixed using a magnetic stirrer for 30 min for effective functional monomer-template interaction. During this process, polymerisable lanthanide complex (0.125 mmol) was added into the miniemulsion medium. Afterwards, the mixture was added to phase 2 in polymerisation reactor, and nitrogen was passed through the mixture for 5 min to remove dissolved oxygen. Then, sodium bisulfite (57.5 mg) and ammonium persulfate (63 mg), were added and polymerisation was continued at 40°C for 1 day. Particles in larger size were removed by centrifuging at 10000 rpm (Allegra-64R Beckman Coulter, maximum RCF at r max (g): 504,000 x g). The melatonin imprinted NPs were washed with DI and DI/ethanol to remove unreacted reagents. Then, the solution was centrifuged at 60000 rpm for 30 min for each step, and NPS were dispersed in fresh washing solution. Finally, the melatonin imprinted NPs were dispersed in DI. Non-imprinted NPs were also synthesised through the same method in the absence of melatonin and N-methacryloyl-L-tryptophan (MATrp), respectively, to provide controls. Characterization molecularly imprinted fluorescent nanoparticles were conducted by atomic force microscopy (AFM) and zeta-size measuments. AFM measrement were done by using ambient AFM (Nanomagnetics Instruments, Oxford, UK) in dynamic mode. 1 μm x 1 μm area were scanned with 1 μm/s scanning rate at 256 × 256 pixels' resolution. For zeta-sizer (NanoS, Malvern Instruments, London, UK), light scattering was done at incidence angle 90° and 25°. The viscosity and the refraction index of deionized water were 0.88 mPas and 1.33, respectively.

### 2.5. Optimisation of Melatonin Detection Conditions

The imprinted fluorescent NPs were examined for melatonin adsorption from aqueous solutions to optimise melatonin detection conditions. The most appropriate pH, temperature, melatonin concentration, ionic, and time were determined in the ranges of 4.0-8.0, 4-40ºC, 0.01-0.5 ng/mL, 0.1-1.0 M, and 15-180 min, respectively. For this step, a continuous agitation at 50 rpm using rotator was maintained during the interaction of the fluorescent NPs with aqueous melatonin solution while varying the conditions given above.

### 2.6. Selectivity Experiments

To examine the selectivity of melatonin imprinted fluorescent NPs, the competitive adsorption of melatonin, serotonin and tryptophan molecules were investigated. Melatonin biosynthesis has four enzymatic steps from the essential dietary amino acid tryptophan follows the serotonin pathway. In this context, analyte solutions with same concentration of 0.03 ng/mL were allowed to interact with melatonin imprinted fluorescent NPs as well as with non-imprinted fluorescent NPs. Herein, changes in fluorescence emission intensity of NPs were measured before and after adsorption. Then, these results were normalised to easily determine the changes in emission intensity. We also analysed the selectivity of the imprinted NPs. The distribution constants ($k_D$), selectivity (k) and the relative selectivity constants (k') were calculated the following equations:

$k_{D,analyte}$ = Intensity*/ Intensity$^0$

$k_{melatonin} = k_{D,melatonin} / k_{D,competitive}$

$k' = k_{MIP} / k_{NIP}$

$k_{D,analyte}$ is the distribution constant of the target metabolite; intensity* is the normalised intensity of target metabolite (intensity*= intensity$^0$ - Intensity$^{analyte}$); intensity$^0$ is emission the intensity of fluorescent NPs (without interaction with any analyte); $k_{melatonin}$ is the selectivity of fluorescent NPs for melatonin against the competitive metabolites and k' is the relative selectivity constants of fluorescent imprinted NPs against fluorescent non-imprinted NPs.

## 3. Results and Discussion

### 3.1. Characterisation of Functional Monomers

The FTIR-ATR spectrum of MATrp is shown in **Figure S1**. The characteristic 3398 cm$^{-1}$ absorption band was due to (secondary amine group) N-H stretching while absorption bands at 3075-3015 cm$^{-1}$ belong to aromatic C-H stretching. C-H stretching band arising from alkyl group is separately determined at 2972 cm$^{-1}$. C=O stretching band of acid is observed at 1657 cm$^{-1}$, and C=C stretching band is at 1577 cm$^{-1}$. C-N stretching aromatic band is at 1488 cm$^{-1}$. Absorption bands at 740-770 cm$^{-1}$ arise from aromatic C-H bending.[36]

The FTIR-ATR spectrum of MAAsp showed a characteristic carbonyl band at 1567 $cm^{-1}$, and the 3395 $cm^{-1}$ absorption band was due to (secondary amine group) N-H stretching. The two C-N symmetric and asymmetric stretching bands were at 1010 and 1388 $cm^{-1}$ as shown in **Figure S1.**[36] The FTIR-ATR spectra confirmed that MATrp and MAAsp were synthesised successfully.

### 3.2. Characterisation of Fluorescent Tb(III):MAAsp Complex

The fluorescent emission bands of Tb(III)-MAAsp complex were (**Figure 1)** 489 nm ($^5D_4$-$^7F_6$), 546 nm ($^5D_4$-$^7F_5$), 584 nm ($^5D_4$-$^7F_4$), and 763 nm ($^5D_4$-$^7F_3$), respectively. These four classical fluorescent emission bands showed that Tb (III) ions were incorporated into complex structure and interaction between ligand (MAAsp) and ion (Tb(III)) were strongly formed[37].

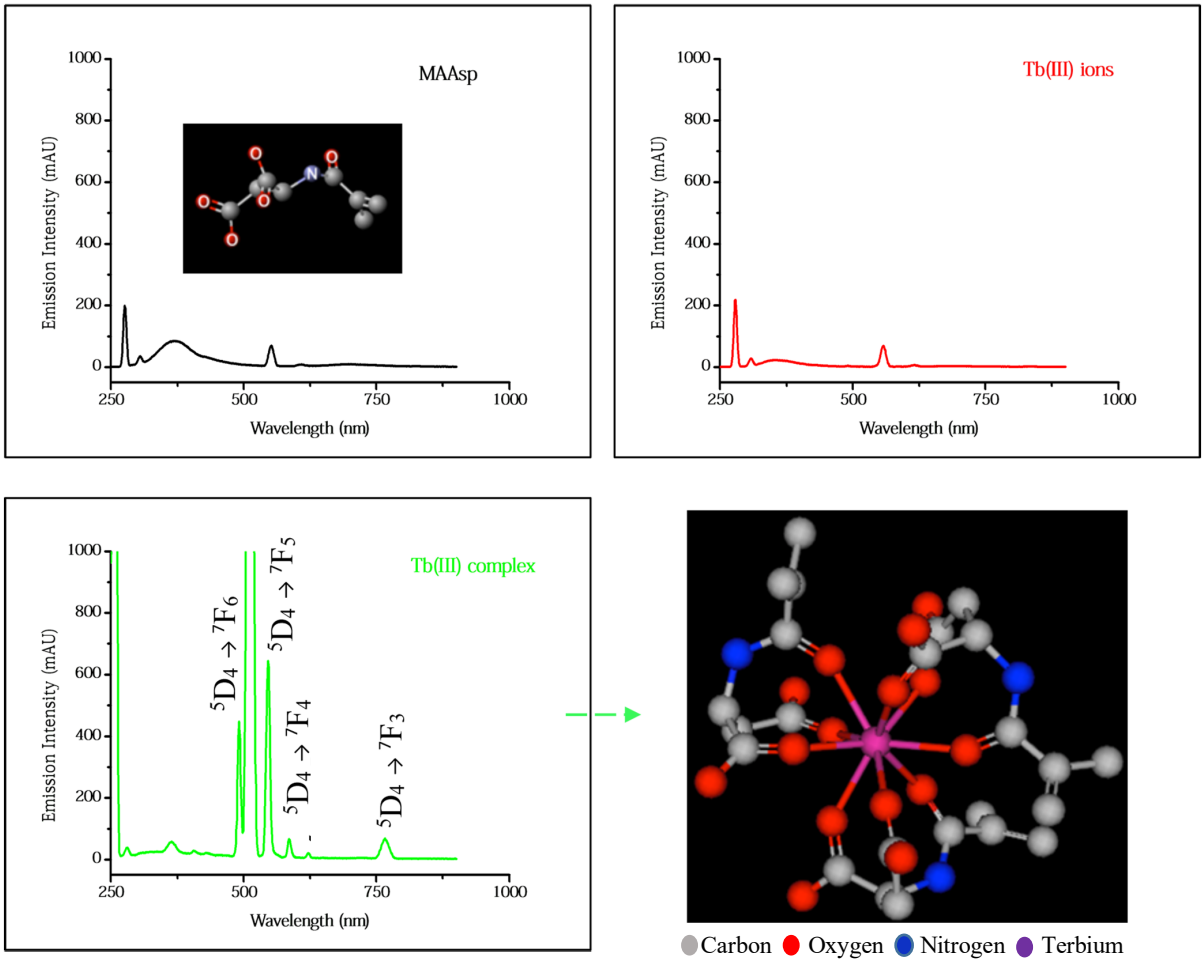


**Figure 1.** Fluorescent emission spectra of Tb(III)-MAAsp complex.

### 3.3. Characterisation of Molecularly Imprinted Fluorescent Nanoparticles

The surface properties and depth of the melatonin imprinted fluorescent NPs were determined by AFM. AFM measuments were performed with AFM (Nanomagnetics Instruments, Oxford, UK) in dynamic mode. The imprinted fluorescent NPs had a spherical shape and was approximately 70 nm **(Figure 2a).**

The particle size and the distribution of the NPs were also measured by Zetasizer (NanoS, Malvern Instruments, London, UK). The size of the melatonin imprinted / non-imprinted NPs are shown in **Figure 2b-c.** The Z-Average hydrodynamic diameter of melatonin imprinted NPs was 63.27 nm with a narrow polydispersity index as 0.093. The Z-Average of melatonin non-imprinted NPs was 73.80 nm with a higher polydispersity index of 0.381 compared to imprinted particles. These results show that the polymerisation technique is appropriate for the synthesis of imprinted NPs with the desired features.

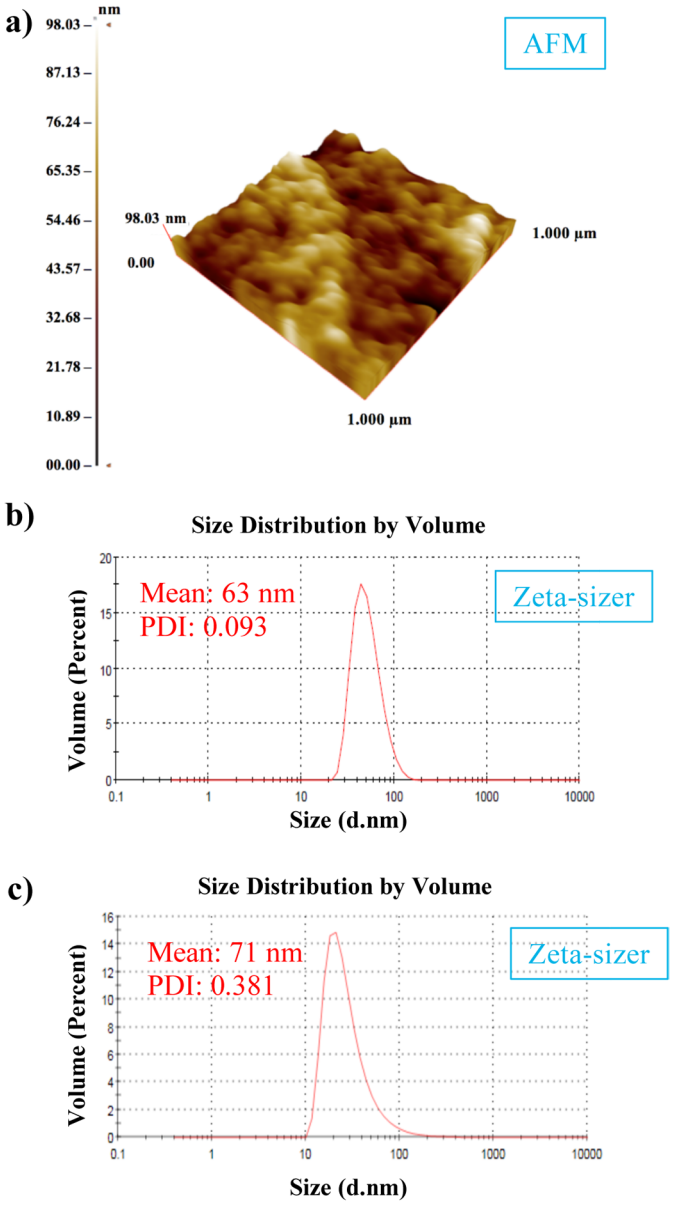


**Figure 2. a)** 3-Dimensional AFM image of imprinted fluorescent nanoparticles; **b)** hydrodynamic size (diameter) of melatonin imprinted nanoparticles and **c)** non-imprinted nanoparticles.

### 3.4. Detection of Melatonin Using Melatonin-Imprinted Fluorescent Nanoparticles

The imprinted fluorescent NPs were examined for melatonin adsorption from aqueous solutions to optimise melatonin detection conditions. The most appropriate pH, temperature, melatonin concentration, ionic, and time were determined in the ranges of 4.0-8.0, 4-40ºC, 0.01-0.5 ng/mL, 0.1-1.0 M, and 15-180 min, respectively. Continuous agitation at 50 rpm using rotator was maintained during the interaction of the fluorescent NPs with aqueous melatonin solution while varying the conditions given above.

The melatonin imprinted fluorescent NPs delivered two linear regions for the detection of melatonin **(Figure 3).** The results suggest that melatonin bound to the melatonin imprinted fluorescent NPs through two different orientations with high affinity. Melatonin imprinted fluorescent NPs showed a linearity of 99% in the concentration range of 0.01-0.05 ng/mL and a linearity of 97% in the concentration range of 0.05-0.5 ng/mL. When the results were plotted as intensity vs log(concentration), only a single linear working range were clearly obeserved with a regression coefficient of 96% (Figure 3b, inset). Limit of detection (LOD) and the limit of quantification (LOQ) were 0.121 and 0.411 pg/mL, respectively.

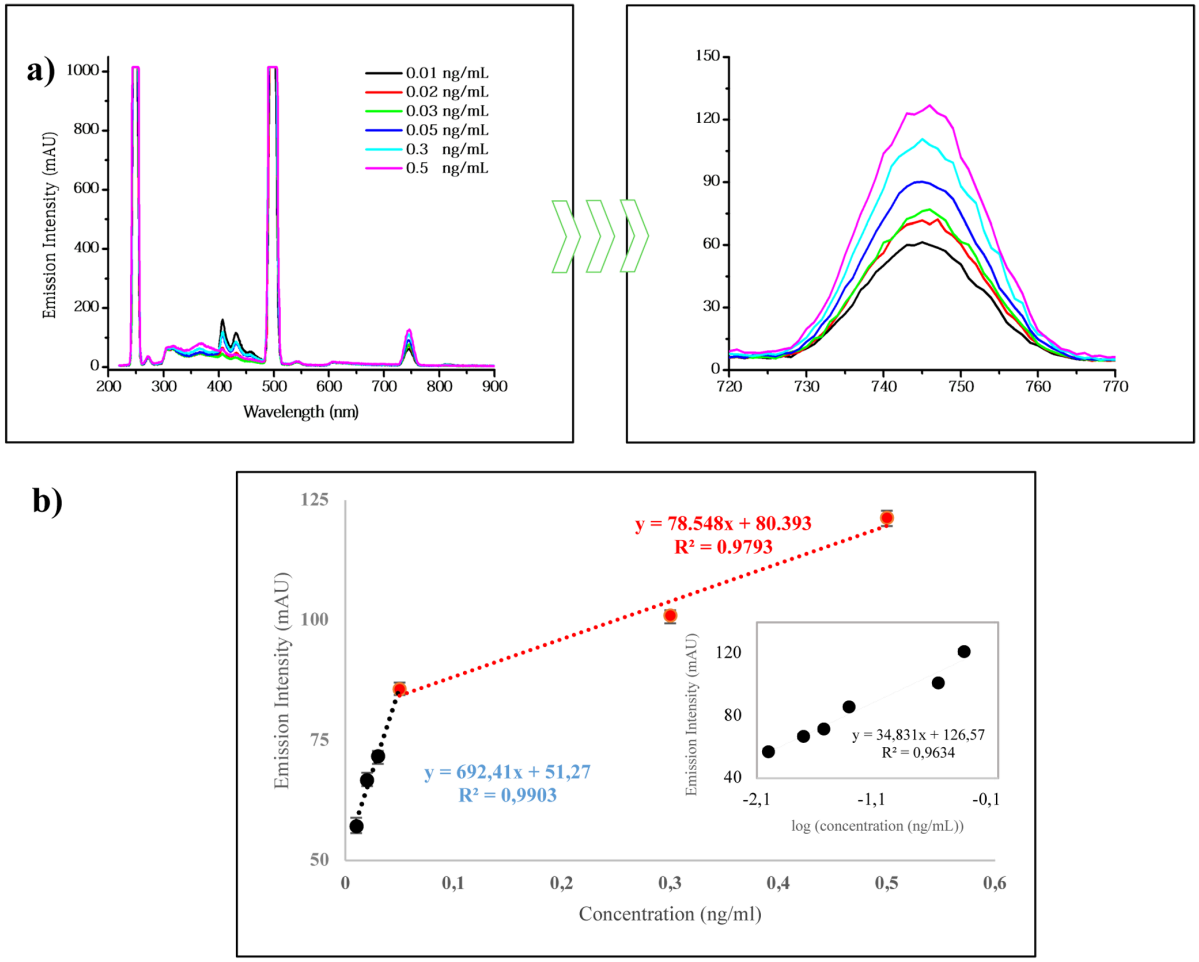


**Figure 3. a)** Fluorescent emission spectra of melatonin adsorption process, **b)** correlation between concentration and emission intensity at 748 nm (excitation wavelength, 248 nm).

In general, the control of melatonin synthesis and secretion, and its synchronisation with the 24-hour body clock are dominated by the light/dark cycle. Endogenous serum melatonin concentration in healthy young adults is in the range of 10 pg/mL typically during daylight hours and at night about 40 pg/mL.[38] Hence, melatonin-imprinted fluorescent NPs can be used for the detection of melatonin over the normal range from 10 to 40 pg/mL and the melatonin value in SAD patients, which reaches about 60 pg/mL and where the secretion is longer in winter than in summer.[39]

The appropriate pH was pH 5.0 **(Figure 4a).** At values below and above pH 5, the adsorption capability of the NPs was significantly decreased. The plausible explanation is that the ligand (tryptophan-based functional monomer, MATrp) is uncharged at pH 5.0 and therefore the hydrophobic interactions at this pH are more selective and via hydrophobic interactions, can achieve higher adsorption capabilities. This is related to structural characteristics of the functional monomer which was used, because molecularly imprinted NPs were synthesised via hydrophobic interactions.

The optimum ionic strength was estimated using NaCl (between 0.1-1.0 M). The ionic strength of the neutral salt added to the medium affects the solubility of the analyte molecules. Ionic strength is determined by the charge and the concentration of cations and anions that form the salt. With increasing concentration of salt there is a decrease in the adsorption of melatonin (**Figure 4b).** This is because of increasing salt concentration melatonin loose the solubility and the interaction between melatonin and NPs increased. The adsorption process reached to the equilibrium value almost in 120 minutes (**Figure 4c).** After this point, the change of adsorption is not significant. This result implies that the adsorption kinetics of fluorescent NPs is relatively rapid. The effect of temperature on the adsorption was determined between 4-40°C **(Figure 4d).** An increase in temperature resulted a significant increase in melatonin adsorption capabilities. These results also imply that the interactions between melatonin and melatonin imprinted fluorescent NPs have a basically hydrophobic character. Hydrophobic interactions depend on the change in the entropy of space and the possibility of hydrophobic interactions between analyte and NPs is enhanced with increasing in the entropy.

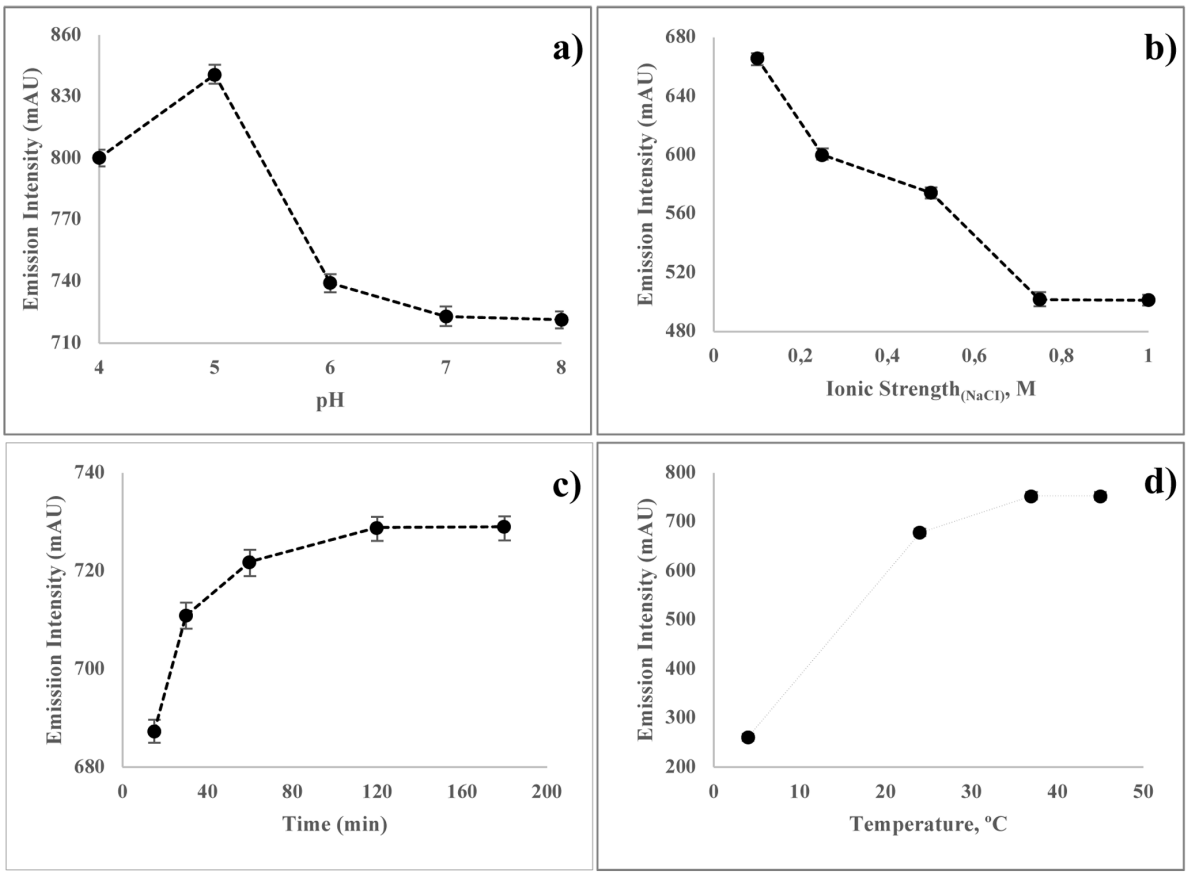


**Figure 4. a)** Effect of pH (melatonin concentration of 0.03 ng/mL, emission values at 748 nm), **b)** Effect of ionic strength (melatonin concentration of 0.03 ng/mL, emission values at 748 nm), **c)** Effect of time (melatonin concentration of 0.03 ng/mL, emission values at 748 nm), **d)** Effect of temperature (melatonin concentration of 0.03 ng/mL, emission values at 748 nm).

### 3.5. Determination of Imprinting Selectivity

In order to evaluate the selectivity of melatonin imprinted fluorescent NPs, the competitive adsorption of melatonin, serotonin and tryptophan molecules were investigated. Herein, the non-imprinted NPs, which were were synthesised for control purpose were also interacted with these analyte molecules. Non-imprinted fluorescent NPs didn't have any significant signal to melatonin whereas they have give higher respose to other molecules, serotonin and tryptophan molecules. On the other hand, the non-imprinted NPs have no selective responses to all of analyte molecules (melatonin, serotonin and tryptophan). As mentioned before, the increase in melatonin concentration results in the enhancing effect on the emission spectra of the fluorescent NPs. However, the presence of melatonin molecules quenches the fluorescent intensity in respect to the plain NPs. Herein, we determined the same results for melatonin when imprinted NPs were used. In addition, the competitive molecules have resulted in a lower decrease in the intensity of the fluorescent NPs in non-selective manner. When the non-imprinted NPs were used, all of the analyte molecules resulted in non-selective decrease in the intensity according to the plain NPs as well. These results stemmed from the

creation of melatonin recognition cavities in the NPs that were close to nanoenvironment of the lanthanide complexes. These molecules behave like a quencher to selectively decrease the intensity. Moreover, the competitor molecules could not directly interact with those cavities which were close to the fluorescent complexes; therefore, their quenching effects are limited. These quenching effects depended on the non-specific surface adsorption which resulted in a bioorganic layer accumulation on the NPs. We have to mentioned that all analyte molecules have an autoflourescent property due to their structural features, i.e. aromatic ring.

As given in the experimental section, the concentrations of all of analyte molecules were kept as 0.03 ng/mL during interaction with melatonin imprinted fluorescent NPs as well as with non-imprinted fluorescent NPs. Then, these results were normalised to assess the changes in emission intensity. The selectivity of the imprinted NPs **(Figure 5)** were compared by calculating distribution constants ($k_D$), selectivity (k) and the relative selectivity constants (k') which were given in **Table. 1**. The changes in emission intensity of fluorescent imprinted NPs are more significant (**Table 1**). The selectivity constants (k) for melatonin molecules determined as 14.97 and 15.63 against serotonin and tryptophan, respectively. These values for non-imprinted fluorescent NPs were also calculated as 0.8175 and 0.6344, respectively. In order to show the selectivity gained by imprinting process, the relative selectivity constant (k') for melatonin illustrates imprinting efficiency, were calculated as 18.31 and 24.64 in respect of the competitor molecules, serotonin and tryptophan, respectively. The imprinting factor (IF) expresses the ratio of specific-to-nonspecific binding for each compound (IF= Emission Intensity$^*_{MIP}$/ Emission Intensity$^*_{NIP}$). The IF values obtained are comparatively given in Table 2. The results indicate that imprinted fluorescent NPs have selective melatonin recognition ability against serotonin and tryptophan. As a conclusion, melatonin imprinted fluorescent NPs could be used in terms of analytical performance and selectivity parameters for the detection of seasonal affective disorder.

**Table 1.** Selectivity parameters for MIP NPs and imprinting factor (IF).

| | MIP | | | NIP | | | | |
|---|---|---|---|---|---|---|---|---|
| | Intensity*, mAU | $k_D$ | k | Intensity*, mAU | $k_D$ | k | k' | IF |
| Melatonin | 621.3 | 0.8965 | | 66.3 | 0.1714 | | | 9.37 |
| Serotonin | 41.5 | 0.0599 | 14.97 | 81.2 | 0.2097 | 0.8175 | 18.31 | 0.51 |
| Tryptophan | 39.8 | 0.0574 | 15.63 | 104.6 | 0.2702 | 0.6344 | 24.64 | 0.38 |

*: Normalised values of intensity. Normalised values are the difference in the fluorescence intensity of fluorescent NPs before and after adsorption.

The intensity of MIP before adsorption: 693 mAU and the intensity of NIP before adsorption 387 mAU.

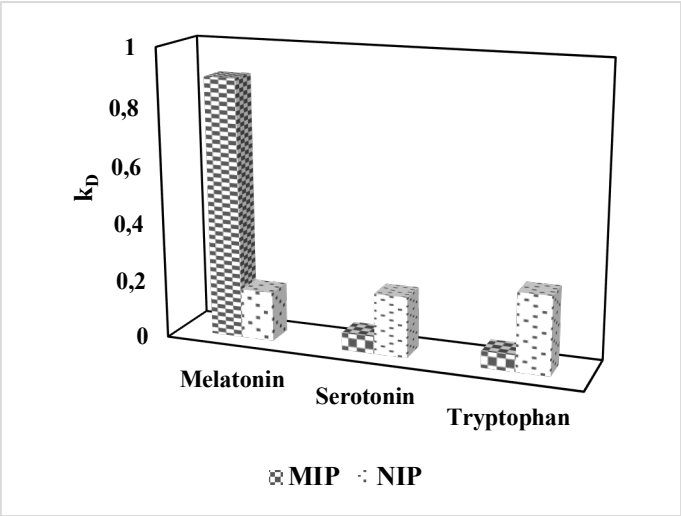


**Figure 5.** Selectivity of the imprinted NPs.

## 4. Conclusions

SAD (winter depression) is labelled by recurrent depressive symptoms during the short photoperiod. Active secretion of melatonin is longer in winter than in summer in patients with SAD (winter depression) due to the lack of sunlight. Changes in of melatonin secretion during this period were have been considered having a role in the pathogenesis of SAD. According to the literature search, there are a few studies based on molecular imprinting to detect and determine melatonin. As can be seen in Table 2, different types of methods based on the molecular imprinting technique and other methods can be used to detect and determine melatonin. In order to provide for the possibility of developing a stable point-of-care test to accompany the therapy, we explored a novel sensing technology using fluorescent imprinted polymer NPs. Efficient and selective fluorescent NPs were obtained by directly inserting lanthanide ion complexes into molecularly imprinted polymeric chains. The fluorescent NPs showed high affinity and selectivity against melatonin, which was 18.3-fold and 24.6-fold higher than that for serotonin and tryptophan. The strategy proposed in this study is a generic, smart and promising approach which in this case delivered LOD and LOQ values of 0.121 and 0.411 pg/mL. This provided a potential nanosensor with high selectivity, high specificity to the target molecules and quite low detection/quantification limits for melatonin, which could be used for melatonin monitoring during the winter period of SAD.

Table 2. Some of studies in the literature for the detection of melatonin.

| Sensing System | Linear dynamic concentration range | LOD | Ref. |
|---|---|---|---|
| Electrochemically initiated co-polymerization of 1H-pyrrole-1-propionic acid (FM1), and 3-(1H-pyrrol-1-yl)-1-propanamine and 2,5-di(2-thienyl)-1H-pyrrole for molecular imprinting analyte | 10-80 μM | 0.14 μM | 40 |
| Molecularly imprinted electrochemical sensing in a microfluidic system | 0-50 pg/mL | ~pM | 41 |
| Molecularly imprinted poly(ethylene-co-vinyl alcohol) coated zinc oxide nanorod arrays | 0-40 pg/mL | ~pg/mL | 42 |
| Aself-assembled Au nanoparticle–MoS2 nanoflake sensing platform | 0.033-10.0 μM | 18.2 nM | 43 |
| A new validated high-performance liquid chromatography with photodiode array detector (HPLC-PDA) | 1.0-40.0 μg/mL | 0.30 μg/mL | 44 |
| $SnO_2$/$SnS_2$ quantum dots | 0.2–1000 μM | 16 nM | 45 |
| Droplet spray ionization mass spectrometry | 0.22–21.50 μM | 0.04 μM | 46 |
| A carbon paste electrode modified with $Al_2O_3$-supported palladium nanoparticles | 6.0 nM- 1.4 mM | 21.6 nM | 47 |
| Lanthanide doped molecularly imprinted nano-architectures | 0.01-0.5 ng/mL | 0.121 pg/mL | This study |


## Acknowledgement

Erdoğan Özgür gratefully acknowledge the financial support for this work was provided by the by The Scientific and Technological Research Council (TUBITAK) of Republic of Turkey (Project number 113 M 919).


## Conflict of interest

The authors declare that they have no conflict of interest.

## References


(1) Yingxin, M.; Xu, Y.; Wang, S.; Wang, L. Luminescent molecularly-imprinted polymer nanocomposites for sensitive detection. *Trends Analyt. Chem.* **2015**, 67, 209-216, DOI: 10.1016/j.trac.2015.01.012.

(2) Nune, S. K.; Gunda, P.; Majeti, B. K.; Thallapally, P. K.; Forrest, M. L. Advances in lymphatic imaging and drug delivery. *Adv. Drug Delivery Rev.* **2011**, 63, 876-885, DOI:

(3) Yao, J., Yang, M.; Duan, Y. Chemistry, biology, and medicine of fluorescent nanomaterials and related systems: new ınsights into biosensing, bioimaging, genomics, diagnostics, and therapy. *Chem. Rev.* **2014**, 114, 6130-6178, DOI: 10.1021/cr200359p.

(4) Kirchner, C.; Lied, T.; Kudera, S.; Pellegrino, T.; Muñoz, J. A.; Gaub, H. E.; Stölzle, S.; Fertig, N.; Parak, W. Cytotoxicity of colloidal CdSe and CdSe/ZnS nanoparticles. *J. Nano Lett.* **2005**, 5, 331-338, DOI: 10.1021/nl047996m.

(5) Burda, C.; Chen, X. B.; Narayanan, R.; El-Sayed, M.A. Chemistry and properties of nanocrystals of different shapes. *Chem. Rev.* **2005**, 105:1025-1102, DOI: 10.1021/cr030063a.

(6) Gao, X. H.; Yang, L. L.; Petros, J. A.; Marshal, F. F.; Simons, J. W.; Nie, S. M. In vivo molecular and cellular imaging with quantum dots. *Curr. Opin. Biotechnol.* **2005**, 16, 63-72, DOI: 10.1385/1-59745-369-2:135.

(7) Yao, S.-L.; Liu, S.-J.; Tian, X.-M.; Zheng, T.-F.; Cao, C.; Niu, C.-Y.; Chen, Y.-Q.; Chen, J.-L.; Huang, H.; Wen, H.-R. A $Zn^{II}$-Based metal-organic framework with a rare tcj topology as a turn-on fluorescent sensor for acetylacetone. *Inorg. Chem.* **2019,** 58, 3578-3581, DOI: 10.1021/acs.inorgchem.8b03316.

(8) Soukka, T.; Härmä, H. In Lanthanide Luminescence: Photophysical, Analytical and Biological Aspects Hänninen, P.; Härmä, H., Eds.; Springer Ser. Fluoresc. **2011**; pp. 89-114.

(9) Bouzigues, C.; Gacoin, T.; Alexandrou, A. Biological applications of rare-earth based nanoparticles. *ACS Nano.* **2011**, 11, 8488-8505, DOI: 10.1021/nn202378b.

(10) Heffern, M. C.; Matosziuk, L. M.; Meade, T. Lanthanide probes for bioresponsive imaging. *J. Chem. Rev.* **2014**, 114, 4496-4539, DOI: 10.1021/cr400477t.

(11) Beaurepaire, E.; Buissette, V.; Sauviat, M. P.; Giaume, D.; Lahlil, K.; Mercuri, A.; Casanova, D.; Huignard, A.; Martin, J. L.; Gacoin, T.; Jean-Pierre Boilot, J. P.; Alexandrou, A. Functionalized fluorescent oxide nanoparticles: artificial toxins for sodium channel targeting and ımaging at the single-molecule level. *Nano Lett.* **2004,** 4, 2079-2083, DOI: 10.1021/nl049105g.

(12) Meyssamy, H.; Riwotzki, K.; Kornowski, A.; Naused, S.; Haase, M. Wet-chemical synthesis of doped colloidal nanomaterials: particles and fibers of $LaPO_4$:Eu, $LaPO_4$: Ce, and $LaPO_4$:Ce,Tb. *Adv. Mater.* **1999**, 11, 840-844, DOI: 10.1002/(SICI)1521-4095(199907)11:10<840::AID-ADMA840>3.0.CO;2-2.

(13) Huignard, A.; Gacoin, T.; Boilot, J. P. Synthesis and properties of colloidal $YVO_4$:Eu phosphors. *Chem. Mater.* **2000**, 12, 1090-1094, DOI: 10.1021/cm990722t.

(14) Wang, L.; Li, P., Wang, L. Luminescent and hydrophilic $LaF_3$-polymer nanocomposite for DNA detection. *Luminescence.* **2008**, 24, 39-44, DOI: 10.1002/bio.1061.

(15) Schäferling, M. The art of fluorescence imaging with chemical sensors. *Angew. Chem. Int. Ed.* **2012**, 51, 3532-3554, DOI: 10.1002/anie.201105459.

(16) Comby, S.; Surender, E. M.; Kotova, O.; Truman, L. K.; Molloy, J. K.; Gunnlaugsson, T. Lanthanide-functionalized nanoparticles as MRI and luminescent probes for sensing and/or imaging applications. *Inorg. Chem.* **2014**, 53, 1867-1879, DOI: 10.1021/ic4023568.

(17) Härmä, H.; Soukka, T.; Lövgren, T. Europium nanoparticles and time-resolved fluorescence for ultrasensitive detection of prostate-specific antigen. *Clin. Chem.* **2001**, 47, 561-568, DOI: 10.1093/clinchem/47.3.561.

(18) Di, W.; Ren, X.; Zhao, H.; Shirahata, N.; Sakka, Y.; Qin, W. Single-phased luminescent mesoporous nanoparticles for simultaneous cell imaging and anticancer drug delivery. *Biomaterials.* **2011**, 32, 7226-7233, DOI: 10.1016/j.biomaterials.2011.06.019.

(19) Oh, W. K.; Jeong, Y. S.; Song, J.; Jang, J. Fluorescent europium-modified polymer nanoparticles for rapid and sensitive anthrax sensors. *Biosens. Bioelectron.* **2011**, 29:172-177, DOI: 10.1016/j.bios.2011.08.013.

(20) Foy, S. P.; Manthe, R. L.; Foy, S. T.; Dimitrijevic, S.; Krishnamurthy, N.; Labhasetwar, V. Optical imaging and magnetic field targeting of magnetic nanoparticles in tumors. *ACS Nano.* **2010,** 4, 5217-5224, DOI: 10.1021/nn101427t.

(21) Whitcombe, M. J.; Kirsch, N.; Nicholls, I. A. Molecular imprinting science and technology: a survey of the literature for the years 2004–2011. *J. Mol. Recognit.* **2014,** 27, 297-401, DOI: 10.1002/jmr.2347.

(22) Schirhagl, R. Bioapplications for molecularly imprinted polymers. *Anal. Chem. 2014,* 86, 250-261, DOI: 10.1021/ac401251j.

(23) Ding, X.; Heiden, P. A. Recent developments in molecularly imprinted nanoparticles by surface imprinting techniques. *Macromol. Mater. Eng.* **2014**, 299, 268-282, DOI: 10.1002/mame.201300160.

(24) Turiel, E.; Martin-Esteban, A. Molecularly imprinted polymers for sample preparation: A review. *Anal. Chim. Acta.* **2010**, 668:87-99, DOI: 10.1016/j.aca.2010.04.019.

(25) Ye, L.; Haupt, K. Molecularly imprinted polymers as antibody and receptor mimics for assays, sensors and drug discovery. *Anal. Bioanal. Chem.* **2004**, 378, 1887-1897, DOI: 10.1007/s00216-003-2450-8.

(26) Turkewitsch, P.; Wabdelt, B.; Darling, G. D.; Powell, W. Fluorescent functional recognition sites through molecular imprinting, A polymer-based fluorescent chemosensor for aqueous cAMP. *Anal. Chem.* **1998**, 70, 2025-2030, DOI: 10.1021/ac980003i.

(27) Li, D. Y.; He, X. W.; Chen, Y.; Li, W. Y.; Zhang, Y. K. Novel hybrid structure silica/CdTe/molecularly imprinted polymer: synthesis, specific recognition, and quantitative fluorescence detection of bovine hemoglobin. *ACS Appl. Mater. Interfaces.* **2013**, 5, 12609-12616, DOI: 10.1021/am403942y.

(28) Zhao, Y. Y.; Ma, Y. X.; Li, H.; Wang, L. Y. Composite QDs@MIP nanospheres for specific recognition and direct fluorescent quantification of pesticides in aqueous media. *Anal. Chem.* **2012**, 84, 386-395, DOI: 10.1021/ac3014934.

(29) Peiser, B. Seasonal affective disorder and exercise treatment: a review. *Biol. Rhythm Res.* **2009**, 40, 85-97, DOI: 10.1080/09291010802067171.

(30) Su, X. C.; Man, B.; Beeren, S.; Liang, H.; Simonsen, S.; Schmitz, C.; Huber, T.; Messerle, B. A.; Otting, G. A Dipicolinic acid tag for rigid lanthanide tagging of proteins and paramagnetic NMR spectroscopy. *J. Am. Chem. Soc.* **2008**, 130, 10486-10487, DOI: 10.1021/ja803741f.

(31) Kielar, F.; Montgomery, C. P.; New, E. J.; Parker, D.; Poole, R. A.; Richardson, S. L.; Stenson, P. A. A mechanistic study of the dynamic quenching of the excited state of europium(III) and terbium(III) macrocyclic complexes by charge- or electron transfer. *Org. Biomol. Chem.* **2007**, 5, 2975-2982, DOI: 10.1039/b709062e.

(32) Butler, S. J.; Parker, D. Anion binding in water at lanthanide centres: from structure and selectivity to signalling and sensing. *Chem. Soc. Rev.* **2013**, 42, 1652-1666, DOI: 10.1039/c2cs35144g.

(33) Hür, D.; Ekti, S. F.; Say, R. N-Acylbenzotriazole mediated synthesis of some methacrylamido amino acids. *Lett. Org. Chem.* **2007**, 4:585-587, DOI: 10.2174/157017807782795556.

(34) Brittain, H.G. Intermolecular energy transfer between lanthanide complexes: 6. Influence of metal-to-ligand ratio on the transfer from terbium (III) to europium (III) complexes of L-histidine. *J. Lumin.,***1979,** 21, 43-51, DOI: 10.1016/0022-2313(79)90033-4.

(35) Starck, M.; Ziessel, R. Multifunctionalized luminescent lanthanide complexes from nonadentate phosphonylated bis-pyrazolyl-pyridine ligands. *Dalton Trans*., **2012,** 41, 13298-13307, DOI: 10.1039/C2DT31181J.

(36) Larkin, J. Infrared and Raman Spectroscopy, Principles and Spectral Interpretation, Elsevier, Amsterdam, Netherland, **2011**.

(37) Gusev, A. N.; Hasegawa, M.; Shimizu, T.; Fukawa, T.; Sakurai, S.; Nishchymenko, G. A.; Shul'gin, V. F.; Meshkova, S. B.; Linert, W. Synthesis, structure and luminescence studies of Eu(III), Tb(III), Sm(III), Dy(III) cationic complexes with acetylacetone and bis(5-(pyridine-2-yl)-1,2,4-triazol-3-yl)propane. Inorganica Chim Acta. 2013, 406, 279–284, DOI: 10.1016/j.ica.2013.04.006

(38) Pandi-Perumal, S. R.; Smits, M.; Spence, W.; Srinivasan, V.; Cardinali, D. P.; Lowe, A. D.; Kayumov, L. Dim light melatonin onset (DLMO): A tool for the analysis of circadian phase in human sleep and chronobiological disorders. *Prog. Neuropsychopharmacol. Biol. Psychiatry.* **2007**, 31, 1-11, DOI: 10.1016/j.pnpbp.2006.06.020.

(39) Checkley, S. A.; Murphy, D. G. M.; Abbas, M.; Marks, M.; Winton, F.; Palazidou, E.; Murphy, D. M.; Franey, C.; Binme, C.; Arendt, J.; Campos Costa, D. Melatonin Rhythms in Seasonal Affective Disorder. *Br. J. Psychiatry.* **1993**, 163, 332-337, DOI: 10.1192/bjp.163.3.332.

(40) Zembrzuska, D.; Kalecki, J.; Cieplak, M.; Lisowski, W.; Borowicz, P.; Noworyta, K.; Sharma, P. S. Electrochemically initiated co-polymerization of monomers of different oxidation potentials for molecular imprinting of electroactive analyte. *Sens. Actuators B Chem.* **2019**, 298, 126884, DOI: 10.1016/j.snb.2019.126884.

(41) Lee, M.-H;, O'Hare, D.; Chen, Y.-L.; Chang, Y.-C.; Yang, C.-H.; Liu, B.-D., Lin, H.-Y. Molecularly imprinted electrochemical sensing of urinary melatonin in a microfluidic system. *Biomicrofluidics.* **2014,** 8, 054115, DOI: 10.1063/1.4898152.

(42) Lee, M.-H.; Thomas, J. L.; Chen, Y.-L.; Lin, C.-F.; Tsai, H.-H.; Juang, Y.-Z.; Liu, B.-D.; Lin, H.-Y. Optical sensing of urinary melatonin with molecularly imprinted poly(ethylene-co-vinyl alcohol) coated zinc oxide nanorod arrays. *Biosens. Bioelectron.* **2013,** 47, 56-61, DOI: 10.1016/j.bios.2013.03.001.

(43) Selvam, S.P.; Hansa, M.; Yun, K. Simultaneous differential pulse voltammetric detection of uric acid and melatonin based on a self-assembled Au nanoparticle–MoS2 nanoflake sensing platform. *Sens. Actuators B Chem.* 2020, 307, 127683, DOI: 10.1016/j.snb.2020.127683.

(44) Vieira, E.S.; Lemos-Senna, E. Application of a new validated HPLC-PDA method for simultaneous determination of curcumin and melatonin in hyaluronic acid-coated nanoemulsions. *J Braz Chem Soc.* **2020,** 31(3), 467-475, DOI: 10.1111/jpi.12624.

(45) Nathiya, D.; Gurunathan, K.; Wilson, J. Size controllable, pH triggered reduction of bovine serum albumin and its adsorption behavior with SnO2/SnS2 quantum dots for biosensing application. *Talanta.* **2020, DOI:** 210,120671, 10.1016/j.talanta.2019.120671.

(46) Jiang, J., Zhang, D., Zhang, H., (...), Zhang, X., Li, N. Rapid determination of melatonin by droplet spray ionization mass spectrometry. *Int. J. Mass Spectrom.* **2019.** 444,116191, DOI: 10.1016/j.ijms.2019.116191.

(47) Soltani, N.; Tavakkoli, N.; Shahdost-fard, F.; Salavati, H.; Abdoli, F. A carbon paste electrode modified with $Al_2O_3$-supported palladium nanoparticles for simultaneous voltammetric determination of melatonin, dopamine, and acetaminophen. *Microchim Acta.* **2019,** 186(8), 540, DOI: 10.1007/s00604-019-3541-3.